The limits of edge bead planarization and surface levelling in spin-coated liquid films

S. Arscott

The limits of edge bead planarization and surface levelling in spin-coated liquid films

Steve Arscott

Institut d'Electronique, de Microélectronique et de Nanotechnologie (IEMN), CNRS UMR8520, The University of Lille, Cité Scientifique, 59652 Villeneuve d'Ascq, France.

E-mail: steve.arscott@univ-lille.fr

Abstract

A model is presented here to predict fluid reflow in a viscous liquid film having time-dependent physical properties. The model is applied to the practical example of the reflow planarization (surface levelling) of 'edge bead' features resulting from the spin coating process. During the reflow planarization of edge beads, the physical properties (surface tension, density and viscosity) of the spin-coated liquid can change over time for several reasons e.g. temperature change, solvent loss, and chemical reaction. The model is compared to experimental findings obtained using two spin-coated viscous liquid films: a drying photoresist (SU-8) and a curing elastomer (polydimethylsiloxane/PDMS). The former reveals the competition between reflow planarization and solvent loss—the latter reveals competition between reflow planarization and polymerization. It is demonstrated that the changing physical properties of the spin-coated viscous liquid, especially the viscosity which can change by orders of magnitudes during these processes, impose limitations on the ultimate achievable practical planarization of the film.

Keywords: spin coating, edge bead, reflow planarization, surface levelling, thin film, SU-8, PDMS

1. Introduction

Understanding reflow planarization [1,2] of a viscous liquid film on a surface [3–6] is important in many practical situations involving coatings [7]. Examples of this range from paints [8] to microelectronics manufacturing [9]. In the latter context, the spin coating a viscous liquid [10] onto a solid surface (e.g. a silicon wafer) is a very common and key process [11]. The ultimate goal of spin coating is the obtainment of a perfectly-uniform thin film of viscous liquid [12] which can be subsequently transformed into a uniform thin solid film by various means such as polymerization, solvent evaporation, chemical reaction etc. There are, however, two main problems with the spin coating process. First, the control of liquid film uniformity over the *majority* of the solid surface—this has been greatly studied and modelled by numerous groups [9,13–20] for the film thicknesses <10 μm due to the evident importance for microelectronics manufacturing [21]. Second, despite bevelling of the wafer edge to avoid sharp edges which can cause resistance to spreading [22], the spin coating process can lead to the accumulation of fluid at the wafer edge [23]—this is commonly called an 'edge bead'. This effect is all the more pronounced for higher viscosity products which are spin-coated at low spin speeds to form 'thick' liquid films, such as thick photoresists [24–26]—something that was, in fact, pointed out sometime ago [27]. Such edge beads are highly undesirable as they have three main detrimental effects. First, they reduce the effective useful 'working area' of the wafer, and by consequence lessen the critical 'device yield' of a technological process—something very undesirable in the microelectronics/microfabrication industries. Second, they can reduce photolithographic resolution by introducing a lithographic proximity effect [28]—this is because the solidified edge bead height is greater than the film thickness in the central part of the wafer. Third, potential wetting of the liquid with the back of the wafer can lead to practical issues such wafer-chuck clamping failure in the subsequent processing—necessitating extra cleaning steps, where possible, to be introduced into the process. Finally, solvents trapped in the drying thick edge beads can cause film cracking and debris ejection onto the wafer surface. Edge beads tend to be relatively thin (<1 μm) and narrow (<1 mm) for low-viscosity (~1 mPa s) photoresists spin-coated at the routine rotation speeds

(~3000-5000 rpm) employed to achieve film thicknesses in the 0.1-10 μm range. In this case, it is a relatively simple task to remove such edge beads using higher spin speed [12], appropriate solvents [29], and other methods [30] making use of modern commercial spin coaters. However, for thicker liquid films, obtained at low spin speeds and/or using high viscosity products, matters are different. There can be problems such as exaggerated film thickness non-uniformity and very poor photolithographic contact in subsequent planar processes. In order to remove edge beads in such thick films, the process engineer may need to resort to physical means, e.g. film compression [31] during film baking or even manual cutting post-baking/curing—however, such approaches are evidently not ideal. Reflow planarization [2–6] is an alternative solution which relies on either surface tension-driven reflow or gravity-driven reflow of the liquid film for a period of time (the planarization time) following spin coating to enable surface levelling. However, during the long-duration planarization required for viscose liquid films—sometimes hours, the principle physical properties of the liquid, e.g. the viscosity, density, and surface tension, can change with time. This can be due to a number of reasons, e.g. solvent loss (in a spin-coated thick film photoresist) or a polymerization reaction during thermal treatment or 'curing' (in a spin-coated silicone liquid elastomer).

Here, the edge bead reflow planarization problem is looked at again by considering the time-varying physical properties of the liquid film undergoing surface levelling. Both surface tension-driven and gravity-driven reflow planarization cases are considered. Simple mathematical models are derived and assumptions are made to be able to apply them to the case of real edge beads obtained when employing spin coating of films. Two practical cases are considered and compared to the model: the reflow planarization of a thick film photoresist (SU-8) whilst drying, and the reflow planarization of a thick film elastomer (polydimethylsiloxane/PDMS) whist curing. In the former case the liquid's properties change due to solvent loss—in the latter case the liquid's properties change due to polymerization. We will see how these changing properties affect the reflow planarization behaviour in the two cases.

2. A model for reflow of a viscous liquid with time-varying properties

Let us start by considering the case of an infinitely wide non-uniform film of liquid in non-equilibrium on an infinitely wide solid surface—shown in Figure 1. We can consider the non-uniformity in the film thickness h to be modelled by the following expression:

$$h = h_\infty + \delta \cos(qx) \tag{1}$$

Where h_∞ is final equilibrium mean value [7] of the film thickness, δ is the amplitude of the perturbation, x is the lateral distance, and $q = 2\pi/\lambda$ where λ is the wavelength of the perturbation. We assume that viscous forces dominate the inertial forces in the fluid $\lambda \gg h_\infty$, i.e. a low Reynold's number. The capillary length κ^{-1} is given by $\sqrt{\gamma/\rho g}$, where γ is the surface tension and ρ is the density. If $\lambda < \kappa^{-1}$ then the surface tension dominates the reflow—in the opposite case ($\lambda > \kappa^{-1}$) gravity dominates the reflow behavior.

We know from fluid dynamics theory that the decay of the amplitude δ of the perturbation with time is given by the following expressions (see Supplementary Material for derivation and full expressions) in the case of either surface tension-driven flow or gravity-driven flow:

$$\ln \delta + C_\gamma^1 = -K_\gamma \int \frac{\gamma(t)}{\eta(t)} dt \tag{2a}$$

$$\ln \delta + C_g^1 = -K_g \int \frac{\rho(t)}{\eta(t)} dt \tag{2b}$$

On the left hand side of the above equations, C_γ^1 and C_g^1 are constants of integration. On the right had sides of the equations, $K_\gamma = h_\infty^3 q^4/3$ (m^{-1}) and $K_g = g h_\infty^3 q^2/3$ ($m^2\ s^{-2}$). The functions $\gamma(t)$, $\rho(t)$, and $\eta(t)$ describe how the surface tension, the density, and the viscosity of the liquid film change with time—for example, during a particular technological process conducted on the liquid film e.g. heating, drying, and polymerization. Note that in the specific case when none of the liquid's physical properties change with time Equations 2a and 2b reduce to:

$$\ln \frac{\delta(t)}{\delta_0} = -\frac{K_{\gamma,g}}{\eta} t \quad (3)$$

Finally becoming the relationship:

$$\delta(t) = \delta_0 e^{-\frac{t}{\tau_{\gamma,g}}} \quad (4)$$

Where the characteristic relaxation times, in the case of surface tension-driven τ_γ and gravity-driven τ_g reflow, are given by the relationships derived by Orchard [3]:

$$\tau_\gamma = \frac{3\eta}{\gamma h_\infty^3 q^4} = \frac{3\eta\lambda^4}{16\pi^4\gamma h_\infty^3} \quad (5)$$

$$\tau_g = \frac{3\eta}{\rho g h_\infty^3 q^2} = \frac{3\eta\lambda^2}{4\pi^2\rho g h_\infty^3} \quad (6)$$

Note that the exponential decay of the fluid perturbation height is also predicted to be valid for aperiodic perturbations of the fluid surface [32]—this allows a comparison of the model with practical perturbations of viscous films such as edge beads which are not periodic.

In order to illustrate these ideas and make comparisons of the model with experimentally-derived edge beads incurred in the spin coating process, two specific practical examples of reflow planarization are studied here. The first is a common thick film photoresist (SU-8) where reflow is in competition with drying. The second is a common elastomer (polydimethylsiloxane/PDMS) where reflow is in competition with polymerization. In the former case, the liquid properties will vary due to solvent loss, in the latter case predominantly due to chemical reaction.

3. Experimental Results

3.1 Planarization of the photoresist SU-8—the competition between reflow and drying

Figure 2 shows a schematic illustration of the evolution of the reflow planarization of an edge bead feature in the case of a drying photoresist such as SU-8. The profile of the edge bead feature directly after spin coating is indicated in Figure 2(a). At this point few solvents have been lost from the SU-8 film and its viscosity is low. As the planarization period progresses, the solvent losses cause the viscosity of the SU-8 to increase as indicated in Figure 2(b)—this decelerates the reflow. Finally towards the end of the planarization period, the solvent loss rate drops and the viscosity of the SU-8 will be very high as shown in Figure 2(c)—this effectively halts the reflow and stops the planarization. In summary, the solvent loss from the photoresist during the planarization period leads to an increase in the viscosity of the film which decelerates the reflow. If the viscosity of the photoresist rises too rapidly (due to a large solvent loss rate), planarization will not be achieved. Let us now turn to some experimentation.

The practical use of reflow planarization of SU-8, e.g. to level its surface and minimize edge beads, has been described by a number of authors [33–37]. It has been stated that SU-8 can be 'self-planarized' due to its 'good mobility' at common baking temperatures (60-100°C) [33]. A 50-100 μm thick layer of SU-8 has been planarized using reflow at 65°C for 15 minutes [34]. In terms of planarization duration, often a 'number of hours' are advised [35]. The planarization of SU-8 can be improved using chemical treatment [36]. Employing several SU-8 layers has been seen to improve planarization [37] as a higher spin speed results in smaller edge beads. However, despite these successful experimental approaches, there has been no quantitative treatment of the reflow of SU-8—let us now try to do this.

The variation of the viscosity of SU-8 is known as a function of solids content (see Supplementary Material) [38]. In order to obtain relationship which describes how the viscosity of SU-8 varies with time, we can carefully weigh the SU-8 photoresist during the evaporation of its solvent (cyclopentanone)—see Supplementary Material. The variation of the density of SU-8 with time can also be deduced from careful experimentation (See Supplementary Material). Following experimentation, Figure 3 shows how the viscosity and density of a spin-coated film of a thick film (~120 μm) of SU-8 changes with time at room temperature.

Several interesting observations can be made from the experimental results presented in detail in the Supplementary Material. The evolution of the solids content S (%) of the SU-8 with time can be accurately modelled by an analytical function known as a Plateau curve (see Supplementary Material), i.e. mass $m \sim \alpha t/(\beta + t)$. The solvent loss (evaporation from the thick film) as a function of time can also be accurately modelled using a Plateau curve. Differentiation of the latter—with respect to time—enables an analytical approximation for the solvent evaporation loss rate to be obtained (see Supplementary Material)—$dm/dt \sim -\alpha\beta/(\beta + t)^2$. The experimentation and analysis (see Supplementary Material) enable approximate expressions for the time-varying viscosity $\eta_{SU-8}(t)$ and density $\rho_{SU-8}(t)$ of the drying SU-8 photoresist to be written down:

$$\eta_{SU-8}(t) = Ae^{\frac{100Bm_{solid}}{\gamma - \frac{\alpha t}{\beta + t}}} \quad (7)$$

$$\rho_{SU-8}(t) = -1805\left(\frac{m_{solid}}{\gamma - \frac{\alpha t}{\beta + t}}\right)^2 + 2827\left(\frac{m_{solid}}{\gamma - \frac{\alpha t}{\beta + t}}\right) + 132 \quad (8)$$

Where the experimentally-obtained numerical values of the constants (A, B, α, β, and γ) for SU-8 can be found in the Supplementary Material. The capillary length of the SU-8 κ_{SU-8}^{-1}~2 mm (see Supplementary Material for the fluid properties of pre-baked SU-8). For spin coated SU-8 films, surface profiling of the edge beads suggest that they have a length of the order of 25 mm. The 'wave length' λ of the edge bead in the model is taken to be the diameter of the wafer (50 mm). As $\lambda > \kappa_{SU-8}^{-1}$, the reflow planarization is dominated by gravity, thus Equations 7 and 8 can be injected into Equation 2b and solved numerically. In a first approximation, we assume the density and viscosity changes to be uniform over the whole thickness of the layer in order to obtain an average viscosity and density of the layer as a function of time. Note that a more accurate solution would be to consider the solvent content to be non-uniform of the resist thickness and hence the viscosity also to be non-uniform [39,40].

Figure 4 shows the variation of the normalized edge bead height as a function of time and SU-8 thickness. The gold curves are obtained by considering a constant viscosity and density. The blue curves

are obtained using the time-varying viscosity and density functions that were experimentally obtained. The thicknesses used in the calculation correspond to the average SU-8 thickness: planarized and non-planarized (see Supplementary Material).

By comparing the gold curves with the blue curves in Figure 4 it is apparent that the increasing density and viscosity of the SU-8 is predicted to greatly affect the reflow planarization behaviour of edge beads irrespective of the resist thickness. The modelling based on time-varying viscosity and density is able to predict the experimentally-obtained values of the normalized edge bead heights (red and green data points). Note that the main cause of the error bars for the points is the measurement of the edge bead's initial height δ_0 directly after spin coating (see Supplementary Material). The model based on time-invariant properties (gold curves) is not able to predict the slow decrease of the normalized edge bead height that is experimentally observed.

3.2 Planarization of polydimethylsiloxane (PDMS)—the competition between reflow and polymerization.

Figure 5 shows a schematic illustration of the evolution of the reflow planarization of an edge bead feature in the case of a curing elastomer such as PDMS. In this case the ongoing polymerization chemical reaction in the elastomer mix during the planarization period leads to an increase in the viscosity of the film which decelerates the reflow. If the viscosity of the PDMS rises too rapidly, planarization will not be achieved. The profile of the edge bead feature directly after spin coating is indicated in Figure 5(a). At this point the polymerization reaction has just begun in the PDMS mixture and its viscosity is low. As the planarization period progresses, the ongoing polymerization reaction [indicated by the crosses in Figure 5(b)] causes the viscosity of the PDMS mixture to increase as indicated in Figure 5(b)—this decelerates the reflow. Finally towards the end of the planarization period, the polymerization nears completion and the viscosity of the PDMS will be very high as shown in Figure 5(c)—as with the SU-8 photoresist above, this effectively halts the reflow and stops the planarization. In summary, the polymerization reaction of the PDMS

mixture during the planarization period leads to an increase in the viscosity of the film which decelerates the reflow. If the viscosity of the PDMS mixture rises too rapidly (due to a large polymerization rate), planarization will not be achieved. Let us now turn to some experimentation.

According to the literature, the viscosity of curing 'elastomer-type' materials can evolve with time in several ways. The viscosity can rise rapidly to a saturation—this has been observed in various silicones drying [41] and sols [42]. The viscosity can rise exponentially, apparently without limit during the process period—this has been seen in some silicones [43–47], epoxy resins [48], and colloidal silica [49]. Finally, the viscosity can rise exponentially to saturation over a long period of time—as seen in some liquid silicones [50] and inks containing ceramic particles [51]. It is well known that the viscosity in a curing PDMS mixture rises due to polymerization which increase the PDMS molecular length [52]. In terms of the density of PDMS, this can also change with temperature [53,54] but to a much less extent than the viscosity. It has been observed that spin-coated PDMS, even when subsequently planarized, can result in large edge beads [55]—something the authors attributed to the increasing viscosity of the mixture during planarization and its impact on reflow.

Analysis of experimental data available in the literature (see Supplementary Material) enables the variation of the viscosity of PDMS with time to be approximated using the following expression:

$$\eta_{PDMS}(t) = \frac{\eta_0^2}{\eta_\infty} e^{\left(\frac{2\ln(\eta_\infty/\eta_0)}{1+e^{-t/\tau_\eta}}\right)} \qquad (9)$$

Where η_0 is the viscosity at $t = 0$ and η_∞ is the viscosity at $t \to \infty$. One can introduce the notion of a '*characteristic viscosity time'* τ_η. Practically, a large τ_η means that the viscosity of the liquid changes relatively slowly with time, whereas a small τ_η means that the viscosity rises rapidly with time.

The variation of the density of the curing PDMS can be measured experimentally (see Supplementary Material) allowing an analytical expression for the variation of the density of curing PDMS with time to be written down:

$$\rho_{PDMS} = \frac{\alpha t}{\beta + t} + \gamma \qquad (10)$$

The experimentally-obtained numerical values of the constants ($\alpha, \beta,$ and γ) for PDMS can be found in the Supplementary Material. Figure 6 shows the evolution of the viscosity and density of curing PDMS at room temperature. Note that compared to the evolution of the viscosity and the density of a drying photoresist, the evolution of these properties can be considered to be uniform thought the thickness of the PDMS as the ongoing polymerization is presumably uniform. For the pre-cured polydimethylsiloxane mixture the capillary length κ_{PDMS}^{-1} ~1.4 mm (see Supplementary Material for the fluid properties of a pre-cured PDMS mixture). For the PDMS, surface profiling of the edge beads suggest that the wavelength λ is of the order of 20-25 mm. Thus, as is the case of the SU-8 photoresist above, the reflow planarization of the PDMS mixture will be dominated by gravity as $\lambda > \kappa_{PDMS}^{-1}$. Equation 9 and 10 can be substituted into Equation 2b and solved numerically.

Figure 7 shows the calculated variation of the normalized edge bead height as a function of time for two different PDMS average thicknesses. As above, the blue curves correspond to modelling of time-variant viscosity and density whereas the gold curves correspond to the model based on constant viscosity and density. The model is able to predict the edge bead height after 24 hours planarization by taking into account the variation of viscosity and density during PDMS curing. Interestingly, the lowest PDMS thickness reveals that when the viscosity rises steeply with time then planarization based on reflow is practically impossible—see Figure 7(a). The model which does not take into account the variation of physical properties (gold curves in Figure 7) does not predict such an occurrence. This is a critical point concerning the predictions of the model—i.e. there are conditions when the viscosity may rise so rapidly that reflow planarization is not possible. The experimental data points in Figure 7 show results of planarized and non-planarized PDMS samples—see the Supplementary Material as to how these experimental results were obtained. The dashed lines in Figure 7 correspond to an exact analytical solution

for the variation of the normalized edge bead height as a function of time which considers an exponentially-rising viscosity and a constant density during curing.

In the case of the viscosity rising exponentially and a constant density or surface tension one can obtain an analytical expression for how the height of the perturbation changes with time. Let us consider that the viscosity η of a polymerizing or drying thick film varies in the following way:

$$\eta(t) = \eta_0 e^{t/\tau_\eta} \tag{11}$$

Where η_0 is the initial viscosity at time $t = 0$. One can introduce the notion of a '*viscosity characteristic time'* τ_η. Practically, a large τ_η means that the viscosity of the liquid changes relatively slowly with time, whereas a small τ_η means that the viscosity rises rapidly with time. If we consider a constant density or constant surface tension then Equations 2a and 2b above can be simplified to:

$$\ln \delta + C^1_{\gamma,g} = -k_{\gamma,g} \int \frac{1}{\eta(t)} dt \tag{12}$$

One can now introduce the notion of k_γ and k_g being the liquid's *pressure coefficients* in either surface tension-driven flow or gravity-driven flow; k_γ and k_g both have the units of pressure, i.e. kg m^{-1} s^{-2} or Pa. They are given by the following expressions: $k_\gamma = \gamma h_\infty^3 q^4/3$ and $k_g = \rho g h_\infty^3 q^2/3$.

The above equation for the viscosity can be substituted and integrated to give the following analytical solution:

$$\ln \frac{\delta(t)}{\delta_0} = \frac{\tau_\eta k_{\gamma,g}\left(e^{-t/\tau_\eta - 1}\right)}{\eta_0} \tag{13}$$

$$\frac{\delta(t)}{\delta_0} = e^{\frac{\tau_\eta k_{\gamma,g}\left(e^{-t/\tau_\eta - 1}\right)}{\eta_0}} \tag{14}$$

This is the equation used to generate the dashed line modelling curves for planarizing PDMS in Figure 7. This expression may be of practical use as suggested by the literature, as some experimental situations

may be approximated by an exponential rise of the viscosity with time and either a constant density or surface tension. In the limit of $t \to \infty$, $\delta(t) \to \delta_\infty$, therefore:

$$\frac{\delta_\infty}{\delta_0} = e^{-\frac{\tau_\eta k_{\gamma,g}}{\eta_0}} \tag{15}$$

A plot of this limit is shown in Figure 8 where the final normalized edge bead height (δ_∞/δ_0) is plotted as a function of the characteristic viscosity time (τ_η). The plot considers an exponentially-rising viscosity with an initial viscosity of 1 Pa s at t = 0. Three values of the pressure constant k_g are used to illustrate the influence of this parameter on the ultimate achievable planarization. The plot reveals that when the characteristic viscosity time is below a certain critical value, 'perfect' planarization or absolute surface levelling is, to all intents and purposes, practically impossible—even if the sample is left planarizing for a very long period of time.

4. Discussion

The following paragraph briefly describes two assumptions made in order to compare the model with the experimental results. It is clear from the equations that the modelling is particularly sensitive to the average film thickness and the width of the perturbation. Read edge beads can have a complex shape [23] but in general are composed of a peak at the wafer edge and trough towards the centre of the wafer [55]. Note that in a first approximation and in order to apply the model to a real edge bead profile the value of λ needs to be assigned. In the case of a large diameter wafer (as used for the PDMS) this is considered to be the total 'width' of the edge bead profile i.e. the peak length plus the trough length—the experimental results provided data for this. In the case of a smaller wafer (as used for the SU-8) this is considered to be half the wafer diameter. Another assumption of the approximation to be able to compare the model with the experimental results concerns the size of the perturbation (the edge bead thickness here) compared to the mean film thickness. In principle, the derivation relies on $\delta \ll h_\infty$ (see the Supplementary Material for

the derivation of Equations 2a and 2b) although in the practical cases presented here this is not strictly the case.

Finally, it can be noted that from a practical point of view there are several competing parameters in the reflow planarization process which is described. For the sake of the following discussion we can assume that the viscous liquid density is constant and that the viscosity of the liquid rises according to a certain mathematical function (e.g. exponential) *at a certain temperature*. In the case of an elastomer such as PDMS, increasing the temperature causes the polymerization rate to increase— this leads to the viscosity rising more rapidly with time. Conversely, the initial viscosity of the elastomer mix will be reduced at the initially-higher curing temperature. Similarly, for a drying photoresist, an increased baking temperature will accelerate solvent losses leading to a more rapid rise in the viscosity with time. Increasing the temperature would cause the initial viscosity of the photoresist to be smaller—but lead to a more rapid rise in the viscosity as drying proceeds. In both cases, liquid reflow could be enhanced by simply increasing the temperature to accelerate the planarization. However, as we have seen increasing the temperature reduces the polymerization time or speeds solvent loss—both effects effectively leading a rapid increase in the viscosity of the liquid with time and thus, counterproductively reducing the reflow. Conversely, reducing the temperature may reduce the polymerization rate and the solvent loss. However, reducing the temperature of the liquid leads to an increase in its viscosity, thus reducing the reflow—again counterproductive to the planarization. Therefore, for a given liquid (pre-polymerized liquid, thick film photoresist, gel etc.) depending on how its physical properties change with both temperature and time, there is like by to be an optimum set of reflow planarization parameters to be found.

5. Conclusions

Surface levelling of a viscous liquid film using reflow planarization can be modelled by a simple one dimensional analytical approach. The model considers time-varying physical properties of the viscous

liquid i.e. viscosity, density, and surface tension. The model is applied to predict the planarization of 'edge bead' features which are an unwanted by-product of the common spin coating process. The model predicts that surface levelling may not be possible under certain circumstances. An example of this is if the viscosity of the viscous film rises too rapidly before the film has time to relax and level. Spin coating and planarization experiments are carried out using two common viscous films: SU-8 photoresist and PDMS elastomer mix. In the former case, the density and viscosity of the SU-8 increase due to solvent loss. In the latter case, the viscosity and density of the PDMS mixture increase due to a polymerization chemical reaction. However, in both cases it is the large rise in the viscosity which dominates the reflow-based surface levelling of edge bead features. It can be noted that the approximate model described here is likely to be more accurate for predicting reflow in elastomers (e.g. PDMS) than photoresists (e.g. SU-8). The reason for this is that the polymerization, and thus the change in viscosity, changes uniformly over the whole of the PDMS film thickness. The viscosity is thus always uniform over the PDMS thickness. This is not the case of the drying SU-8 where solvent loss is greater at the surface than at the wafer-SU-8 interface. The viscosity of the SU-8 is therefore higher at the SU-8/air interface than at the SU-8/wafer interface meaning that it varies over the thickness of the film. Both the modelling and experiments demonstrate a clear competition between the reflow of the viscous film and the effects which cause the physical properties (predominantly the viscosity) of the viscous film to change with time, e.g. solvent loss or polymerization. It is both predicted and experimentally observed that in certain cases the complete planarization of the spin-coated viscous film is, to all intents and purposes, practically impossible if the viscosity rises too rapidly with time compared to the film reflow relaxation time.

Acknowledgements

The work was in part funded by the French 'Renatech' network.

ORCID iD

Steve Arscott https://orcid.org/0000-0001-9938-2683

References

[1] Ahmed G, Sellier M, Lee Y C, Jermy M and Taylor M 2015 Rheological effects on the levelling dynamics of thin fluid films *Int. J. Numer. Methods Heat Fluid Flow* **25** 1850–67

[2] Kirchner R and Schift H 2019 Thermal reflow of polymers for innovative and smart 3D structures: A review *Mater. Sci. Semicond. Process.* **92** 58–72

[3] Orchard S E 1963 On surface levelling in viscous liquids and gels *Appl. Sci. Res.* **11** 451–64

[4] Stillwagon L E 1987 Planarization of Substrate Topography by Spin Coating *J. Electrochem. Soc.* **134** 2030–7

[5] Bornside D E, Brown R A, Mittal S and Geyling F T 1991 Global planarization of spun-on thin films by reflow *Appl. Phys. Lett.* **58** 1181–3

[6] Stillwagon L E and Larson R G 1990 Leveling of thin films over uneven substrates during spin coating *Phys. Fluids Fluid Dyn.* **2** 1937–44

[7] Weinstein S J and Ruschak K J 2004 Coating Flows *Annu. Rev. Fluid Mech.* **36** 29–53

[8] Overdiep W S 1986 The levelling of paints *Prog. Org. Coat.* **14** 159–75

[9] Washo B D 1977 Rheology and Modeling of the Spin Coating Process *IBM J. Res. Dev.* **21** 190–8

[10] Scriven L E 1988 Physics and Applications of DIP Coating and Spin Coating *MRS Proc.* **121** 717–29

[11] Madou M J 2002 *Fundamentals of Microfabrication: The Science of Miniaturization, Second Edition* (CRC Press)

[12] Emslie A G, Bonner F T and Peck L G 1958 Flow of a Viscous Liquid on a Rotating Disk *J. Appl. Phys.* **29** 858–62

[13] Meyerhofer D 1978 Characteristics of resist films produced by spinning *J. Appl. Phys.* **49** 3993–7

[14] Flack W W, Soong D S, Bell A T and Hess D W 1984 A mathematical model for spin coating of polymer resists *J. Appl. Phys.* **56** 1199–206

[15] Bornside D E, Macosko C W and Scriven L E 1987 Modeling of spin coating. *J. Imaging Technol.* **13** 122–30

[16] Lawrence C J 1988 The mechanics of spin coating of polymer films *Phys. Fluids* **31** 2786–95

[17] Lawrence C J and Zhou W 1991 Spin coating of non-Newtonian fluids *J. Non-Newton. Fluid Mech.* **39** 137–87

[18] Yonkoski R K and Soane D S 1992 Model for spin coating in microelectronic applications *J. Appl. Phys.* **72** 725–40

[19] Hall D B, Underhill P and Torkelson J M 1998 Spin coating of thin and ultrathin polymer films *Polym. Eng. Sci.* **38** 2039–45

[20] Eres M H, Weidner D E and Schwartz L W 1999 Three-Dimensional Direct Numerical Simulation of Surface-Tension-Gradient Effects on the Leveling of an Evaporating Multicomponent Fluid *Langmuir* **15** 1859–71

[21] Kelso M V, Mahenderkar N K, Chen Q, Tubbesing J Z and Switzer J A 2019 Spin coating epitaxial films *Science* **364** 166–9

[22] Oliver J F, Huh C and Mason S G 1977 Resistance to spreading of liquids by sharp edges *J. Colloid Interface Sci.* **59** 568–81

[23] Shiratori S and Kubokawa T 2015 Double-peaked edge-bead in drying film of solvent-resin mixtures *Phys. Fluids* **27** 102105–21

[24] Lorenz H, Despont M, Fahrni N, LaBianca N, Renaud P and Vettiger P 1997 SU-8: a low-cost negative resist for MEMS *J Micromech Microeng* **7** 121–4

[25] O'Brien J, Hughes P J, Brunet M, O'Neill B, Alderman J, Lane B, O'Riordan A and O'Driscoll C 2001 Advanced photoresist technologies for microsystems *J. Micromechanics Microengineering* **11** 353–8

[26] Zhou Z-F and Huang Q-A 2017 Modeling and Simulation of SU-8 Thick Photoresist Lithography *Micro Electro Mechanical Systems* vol 2, ed Q-A Huang (Singapore: Springer Singapore) pp 1–31

[27] Ciarlo D R and Ceglio N M 1980 Ultrathick Photoresist Processing *Developments in Semiconductor Microlithography V* Developments in Semiconductor Microlithography V ed J W Dey (San Jose) pp 64–73

[28] Thompson L F, Willson C G and Bowden M J 1994 *Introduction to microlithography* (Washington, DC: American Chemical Society)

[29] Jekauc I, Watt M, Hornsmith T and Tiffany J 2004 Necessity of chemical edge bead removal in modern-day lithographic processing Microlithography 2004 ed J L Sturtevant (Santa Clara, CA) p 1255

[30] Chaplick V, Degenkolb E, Elliott D, Harte K, Millman, Jr. R and Tardif M 2010 Analysis of photoresist edge bead removal using laser light and gas SPIE Advanced Lithography ed M V Dusa and W Conley (San Jose, California) p 76403J

[31] Yurgens A 2019 Making thick photoresist SU-8 flat on small substrates *J Micromech Microeng* **29** 017001–5

[32] Chivilikhin S A 1985 Relaxation of a small local perturbation of the surface of a viscous fluid in the stokes approximation *Fluid Dyn.* **20** 450–4

[33] Lin C-H, Lee G-B, Chang B-W and Chang G-L 2002 A new fabrication process for ultra-thick microfluidic microstructures utilizing SU-8 photoresist *J Micromech Microeng* **12** 590–7

[34] Tuomikoski S and Franssila S 2004 Wafer-Level Bonding of MEMS Structures with SU-8 Epoxy Photoresist *Phys. Scr.* **T114** 223–6

[35] Campo A del and Greiner C 2007 SU-8: a photoresist for high-aspect-ratio and 3D submicron lithography *J Micromech Microeng* **17** R81–95

[36] Lee H, Lee K, Ahn B, Xu J, Xu L and Oh K W 2011 A new fabrication process for uniform SU-8 thick photoresist structures by simultaneously removing edge bead and air bubbles *J. Micromechanics Microengineering* **21** 125006–8

[37] Malekabadi A and Paoloni C 2016 UV-LIGA microfabrication process for sub-terahertz waveguides utilizing multiple layered SU-8 photoresist *J. Micromechanics Microengineering* **26** 095010–8

[38] Mitra S K and Chakraborty S 2012 *Microfluidics and nanofluidics handbook: fabrication, implementation, and applications* (Roca Raton, FL: CRC Press)

[39] Münch A, Please C P and Wagner B 2011 Spin coating of an evaporating polymer solution *Phys. Fluids* **23** 102101–12

[40] Hennessy M G, Breward C J W and Please C P 2016 A Two-Phase Model for Evaporating Solvent-Polymer Mixtures *SIAM J. Appl. Math.* **76** 1711–36

[41] Kontopoulou M, Kaufman M and Docoslis A 2009 Electrorheological properties of PDMS/carbon black suspensions under shear flow *Rheol. Acta* **48** 409–21

[42] Zhang X-X, Xia B-B, Ye H-P, Zhang Y-L, Xiao B, Yan L-H, Lv H-B and Jiang B 2012 One-step sol–gel preparation of PDMS–silica ORMOSILs as environment-resistant and crack-free thick antireflective coatings *J. Mater. Chem.* **22** 13132–40

[43] Schneider F, Draheim J, Kamberger R and Wallrabe U 2009 Process and material properties of polydimethylsiloxane (PDMS) for Optical MEMS *Sens. Actuators Phys.* **151** 95–9

[44] Wang Y, Zheng H, Hu R and Luo X 2014 Modeling on phosphor sedimentation phenomenon during curing process of high power LED packaging *J. Solid State Light.* **1** 2–9

[45] Yu X, Xie B, Shang B, Chen Q and Luo X 2016 A Cylindrical Tuber Encapsulant Geometry for Enhancing Optical Performance of Chip-on-Board Packaging Light-Emitting Diodes *IEEE Photonics J.* **8** 1–9

[46] Shu W, Yu X, Hu R, Chen Q, Ma Y and Luo X 2017 Effect of the substrate temperature on the phosphor sedimentation of phosphor-converted LEDs *2017 18th International Conference on*

Electronic Packaging Technology (ICEPT) 2017 18th International Conference on Electronic Packaging Technology (ICEPT) (Harbin, China: IEEE) pp 398–401

[47] Snell K, Lopez I, Louie B, Kiessling R and Sanii B 2019 Drawing and Hydrophobicity-patterning Long Polydimethylsiloxane Silicone Filaments *J. Vis. Exp.* 58826

[48] Wu Z, Huang R, Huang C and Li L 2017 Properties of radiation stable insulation composites for fusion magnet *J. Phys. Conf. Ser.* **897** 012004–6

[49] Agapoulaki G I and Papadimitriou A G 2018 Rheological Properties of Colloidal Silica Grout for Passive Stabilization Against Liquefaction *J. Mater. Civ. Eng.* **30** 04018251

[50] Sötebier C, Michel A and Fresnais J 2012 Polydimethylsiloxane (PDMS) Coating onto Magnetic Nanoparticles Induced by Attractive Electrostatic Interaction *Appl. Sci.* **2** 485–95

[51] Zocca A, Franchin G, Elsayed H, Gioffredi E, Bernardo E and Colombo P 2016 Direct Ink Writing of a Preceramic Polymer and Fillers to Produce Hardystonite ($Ca_2ZnSi_2O_7$) Bioceramic Scaffolds ed A Bandyopadhyay *J. Am. Ceram. Soc.* **99** 1960–7

[52] Zolper T J, Jungk M, Marks T J, Chung Y-W and Wang Q 2013 Modeling Polysiloxane Volume and Viscosity Variations With Molecular Structure and Thermodynamic State *J. Tribol.* **136** 011801–12

[53] Barlow A J, Harrison G and Lamb J 1964 Viscoelastic relaxation of polydimethylsiloxane liquids *Proc. R. Soc. Lond. Ser. Math. Phys. Sci.* **282** 228–51

[54] Dee G T, Ougizawa T and Walsh D J 1992 The pressure-volume-temperature properties of polyethylene, poly(dimethyl siloxane), poly(ethylene glycol) and poly(propylene glycol) as a function of molecular weight *Polymer* **33** 3462–9

[55] Baetens T and Arscott S 2019 Planarization and edge bead reduction of spin-coated polydimethylsiloxane *J. Micromechanics Microengineering*

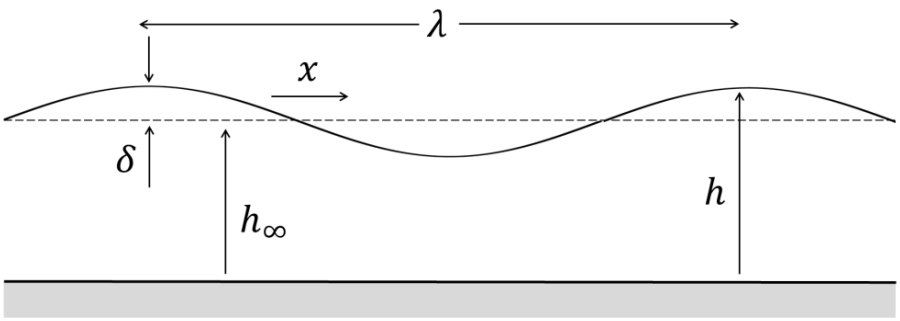

Figure 1 Waves on the surface of a thin film of viscose liquid resting a solid surface (light grey). The thickness of the film is h, the thickness of the perturbation is δ, the equilibrium mean thickness of the film is h_∞, and the wavelength of the perturbation is λ.

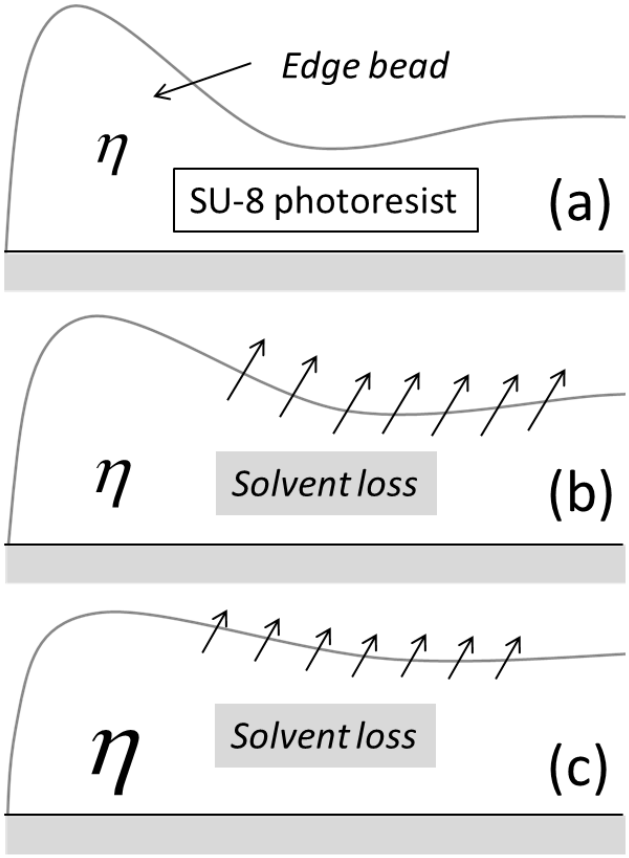

Figure 2 Schematic illustrations showing the effect of increasing viscosity on the evolution of the reflow planarization 'surface levelling' of an edge bead feature in the case of a drying photoresist such as SU-8. (a) The edge bead profile directly following spin coating—the SU-8 has a small viscosity η, (b) during planarization where solvent loss rate is large (indicated by the arrows)—the SU-8 has an increased viscosity, and (c) towards the end of the planarization where the solvent loss rate is small—the SU-8 has a large viscosity.

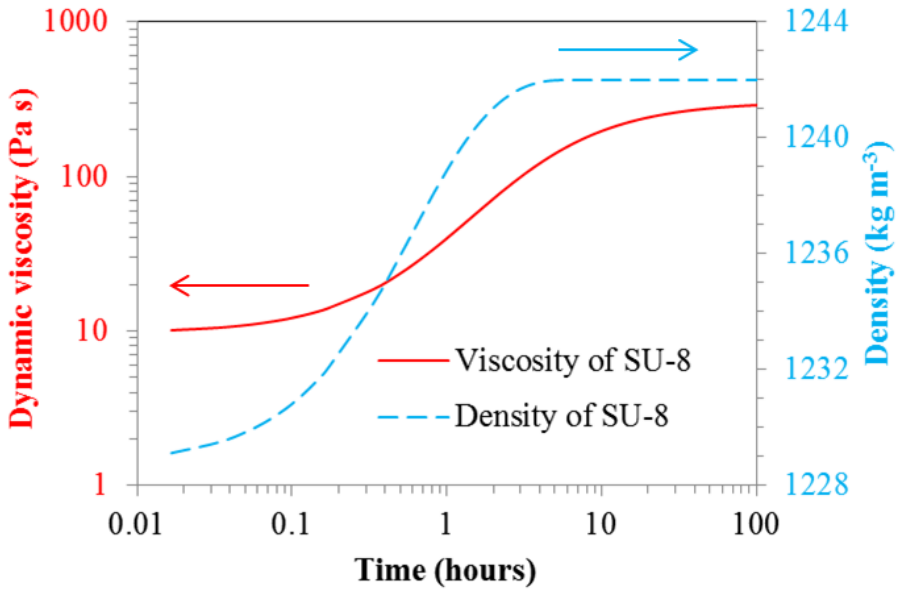

Figure 3 The variation of the viscosity (solid red line) and density (dashed blue line) of a drying SU-8 photoresist film at room temperature. In this case the SU-8 is the '2035' grade. The SU-8 was spin coated (at 1000 rpm) onto a silica disc having a diameter of 50 mm. The SU-8 film thickness is ~120 µm.

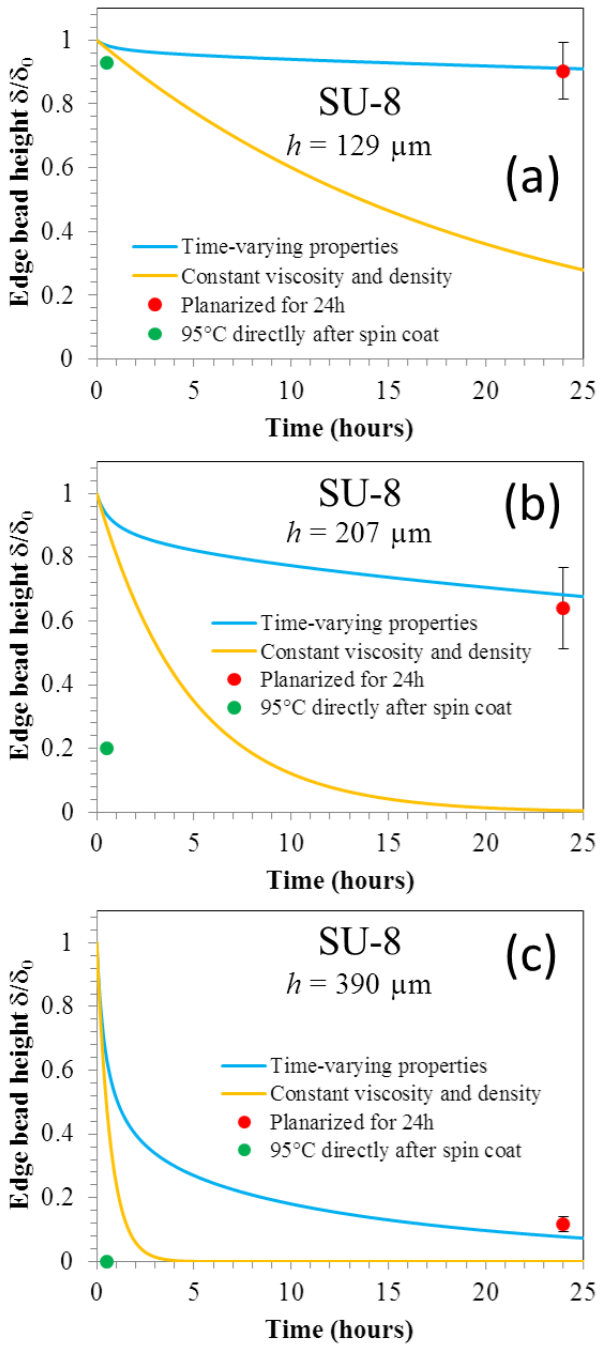

Figure 4 Room temperature reflow planarization of drying SU-8. The variation of the normalized height (δ/δ_0) of the edge bead is plotted as a function of time for different SU-8 thicknesses (a) 129 µm, (b) 207 µm, and (c) 390 µm. The SU-8 is 2035 grade commercially-available from MicroChem, USA. The solid blue lines correspond to the analytical model with time-varying viscosity and density. The solid gold line corresponds to constant physical properties. The red data points correspond to SU-8 samples which were

planarized for 24 hours. The green data points correspond to SU-8 samples which were annealed at 95°C directly following the spin coating step. The SU-8 thicknesses used for the modelling are the average measured thickness for planarized and non-planarized samples.

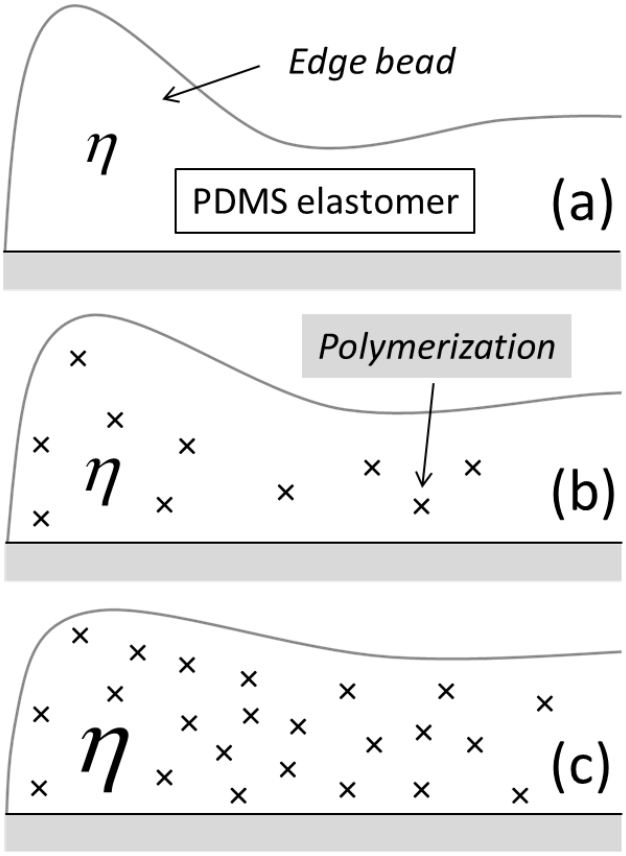

Figure 5 Schematic illustrations showing the effect of increasing viscosity on the evolution of the reflow planarization 'surface levelling' of an edge bead feature in the case of a polymerizing elastomer such as PDMS. (a) The edge bead profile directly following spin coating—the PDMS mixture has a small viscosity η, (b) during planarization where the polymerization reaction (indicated by the crosses) is partially complete—the PDMS mixture has an increased viscosity, and (c) towards the end of the planarization where the polymerization reaction is near completion—the PDMS has a large viscosity.

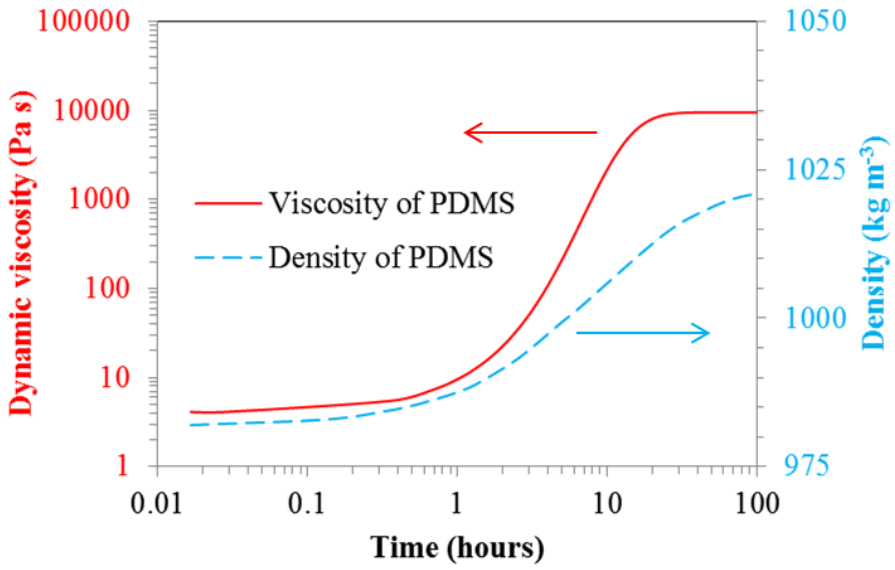

Figure 6 The variation of the viscosity (solid red line) and density (dashed blue line) of curing PDMS at room temperature. In this case the PDMS is Sylgard 184 (Dow Corning, USA). The PDMS was spin coated (at 350 rpm) onto a silica disc having a diameter of 76.2 mm. The thickness of the PDMS is ~370 μm.

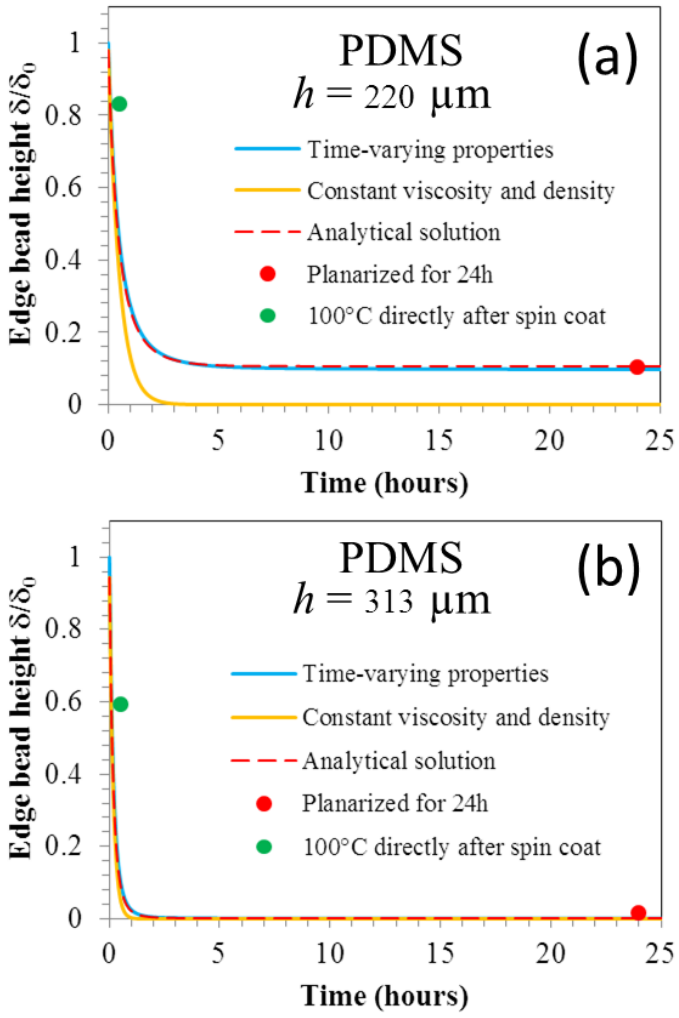

Figure 7 Room temperature reflow planarization of curing polydimethylsiloxane (PDMS). The variation of the normalized height (δ/δ_0) of the edge bead is plotted as a function of time for different PDMS thicknesses. The PDMS is commercially-available Sylgard 184 (Dow Corning, USA) with a base/curing agent mixing ratio of 10:1. The solid blue lines correspond to the analytical model with time-varying viscosity and density. The solid gold line corresponds to a model with constant physical properties. The

red data points correspond to PDMS samples which were planarized for 24 hours. The green data points correspond to PDMS samples which were annealed at 100°C directly following the spin coating step. The dashed red line corresponds to the exact analytical solution obtained if we consider an exponentially-rising viscosity and a constant density (see Supplementary Material).

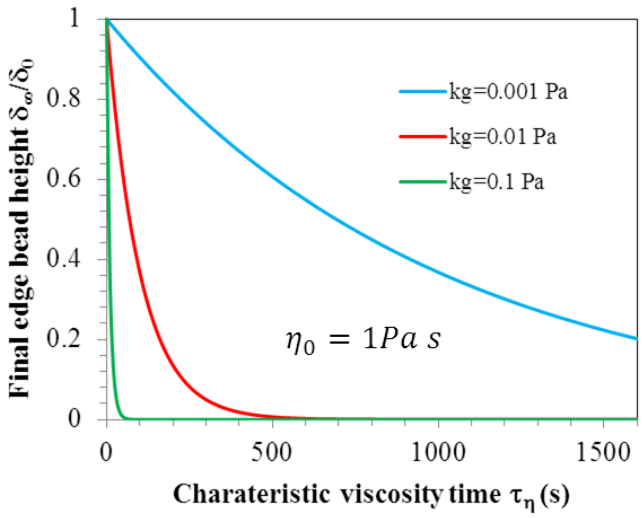

Figure 8 A plot of the final normalized edge bed height (δ_∞/δ_0) as a function of the characteristic viscosity time (τ_η) for different values of the constant k_g. The values of k_g are 1×10^{-3} Pa, 1×10^{-2} Pa, and 1×10^{-1} Pa. The reflow is gravity-driven. The value of initial viscosity η_0 = 1 Pa s. During the reflow planarization, the viscosity varies as $\eta(t) = \eta_0 e^{t/\tau_\eta}$.